

Microvascular morphology of bone in arthrosis

Scanning electron microscopy in rabbits

Shu-zheng He¹, Zhenhua Xiu¹, Ebbe Stender Hansen² and Cody Bünge²

The morphology of the bone microvasculature in rabbit arthrosis was studied by scanning electron microscopy (SEM) and related to changes in intraosseous pressure (IOP) and phlebographic appearance.

Unilateral gonarthrosis was induced in 34 rabbits by immobilization of one knee in extension with a plastic splint for 5 weeks. Bilateral IOP recording in a subgroup of 12 rabbits demonstrated hypertension in arthrosis of 22 ± 2.9 mmHg compared with 11 ± 4.7 mmHg in control knees. Intraosseous phlebography in 13 rabbits showed a dilated vascular bed with prolonged clearance of contrast media. The morphology of normal microvasculature by SEM of intravascular methyl methacrylate casts in 9 rabbits was characterized by well-defined and well-demarcated sinusoids with only a few arteriovenous shunts, whereas in arthrosis substantial changes included fusion of sinusoids, leakage of cast material through the sinusoid walls, and development of numerous shunts.

The study demonstrated profound microvascular morphologic changes that may reflect a vascular genesis for some of the bone changes in arthrosis.

The vascular changes in arthrosis include arterial hyperplasia (Harrison et al. 1953) and venous engorgement (Arnoldi et al. 1972). The presence of intraosseous hypertension, which has been related to pain, may be secondary to synovial effusion as demonstrated both experimentally and clinically (Arnoldi and Reimann 1979). Recent studies of intraosseous gases by mass spectrometry and pressure measurements showed hypoxia and hypercapnia in arthrosis (Pedersen et al. 1988), which might be associated with osteonecrosis. However, the pathogenetic role of intraosseous hypertension has never been settled, and the microstructural changes of the vessels and their relation to altered bone metabolism

have never been analyzed. The development of scanning electron microscopy (SEM) has provided a tool for evaluation of the three-dimensional architecture of microvascular beds (Murakami 1971, 1978). A number of experimental models of arthrosis have showed pathologic changes similar to those found in humans (Telhag and Lindberg 1972, Langenskiöld et al. 1979).

We have analyzed the microvascular changes by SEM of intravascular casts in an established arthrosis model, and have compared the observations with intraosseous pressure changes and phlebographic appearance.

Material and methods

34 rabbits (4 months old, weighing 2.4 ± 0.4 kg) comprised the material. Unilateral arthrosis of the knee was induced in 34 rabbits by immobilization of one knee in extension with a plastic splint for 5 weeks. Right or left knee was selected randomly for splintage; the contralateral knee served as a control.

Orthopedic Department of the Teaching Hospital, and Laboratory at the Clinical Institute¹, Henan Medical University, Henan Province, P.R. China, and Orthopedic Hospital², Århus, Denmark

Correspondence: Dr. Shu-zheng He, Orthopedic Hospital, Randersvej 1, DK-8200 Århus N, Denmark

Phlebography. Intraosseous phlebography was performed in 13 rabbits. Under general i.v. anesthesia (urethane 20 percent, 1g/kg), anteroposterior and lateral radiography of the knees were performed, followed by intraosseous phlebography. A self-tapping needle was inserted through the cortex of the tibial metaphysis. Hypaque® (45 percent, 0.5 mL) was injected through the cannula for 25 s to display the pattern of medullary veins, sinusoids, and adjacent deep veins. X-ray exposures were obtained 5, 10 and 15 s after contrast injection.

Intraosseous pressure. IOP was measured in 12 rabbits. Under general anesthesia (as above), a cannula (I.D. 0.95 mm, O.D. 1.5 mm) was inserted in the upper tibia 5 mm medial to the tibial tuberosity. After flushing gently with heparinized saline solution, the cannula was connected to a pressure recording system (XWT-206, Xinwa Medical Instrument Company, P.R. China) via a manometer catheter. IOP was recorded with a paper speed of 15 cm/min.

Microvascular casting. An intramedullary microvascular cast of the lower extremities was prepared in 9 rabbits. Under general urethane anesthesia, the aorta and the inferior caval vein were isolated. The aorta was catheterized with a 5F polyethylene catheter and ligated, and the caval vein was opened to permit free venous outflow into the abdominal cavity. Nine parts methyl methacrylate were mixed with 1 part methacrylate, and benzoyl peroxide was added to 6 percent of the total volume. This solution was gradually heated for 5–8 min at 80 °C until the viscosity of the semipolymerized methyl methacrylate was similar to that of a 30 percent glycerin solution. It was then cooled immediately to room temperature.

The aorta was first flushed with Ringer's solution to remove all blood from the lower extremities. The semipolymerized methyl methacrylate was mixed with 10 percent N,N-dimethylaniline and injected immediately at an injection pressure of 90 mmHg until the caval vein was filled.

The animals were then killed with an anesthetic overdose. After polymerization the upper tibiae were harvested and demineralized in a solution of 10 percent formic acid and 10 percent hydrochloric acid for 7 to 10 days followed by maceration for 24 to 48 h in 20 percent sodium hydroxide, and finally washed in running distilled water. The microvascular cast was trimmed under a binocular light microscope and dried at 37 °C for 24 h after further washing in distilled water.

SEM analysis. An acceleration voltage of 25 kV was usually suitable for the SEM analysis. The

proximal 5-cm tibial microvascular cast was studied by SEM at magnifications of 20×–1500× in standardized epiphyseal and metaphyseal areas corresponding to the phlebography.

Results

Pathology. The immobilized knees had severe arthrotic changes including stiffness, contracture, muscle atrophy, and thickening of the joint capsule.

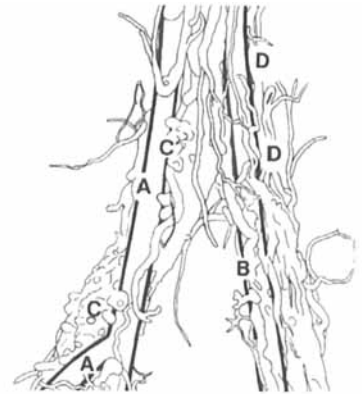
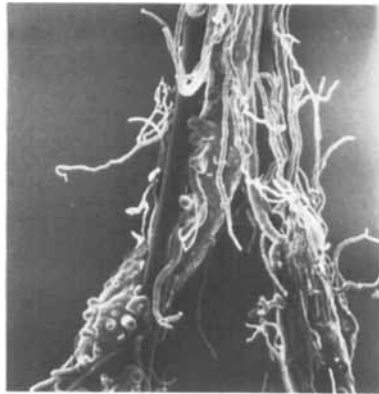
Radiography. Radiography showed osteophyte formation, subchondral sclerosis, and narrowing of the joint space. These pathologic features have previously been described in detail (Langenskiöld 1979, Finsterbush and Friedman 1975).

Intraosseous pressure and phlebography. The IOP of immobilized knees was higher (22.4 ± 2.9 mmHg) than that of control knees (11.2 ± 4.7 mmHg; $P < 0.001$). Phlebography showed venous engorgement with distension of subchondral as well as medullary vessels.

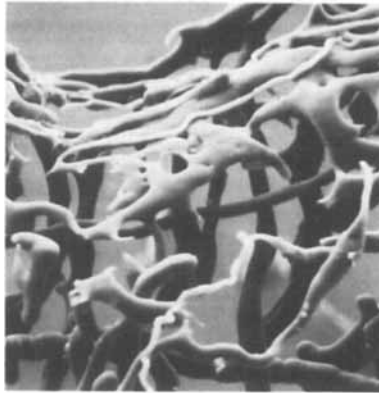
Microvascular morphology. Normal bone (Figures 1 and 2). After entering the medullary canal, the nutrient artery immediately divides into an ascending and a descending branch. The ascending artery is short and gives rise to central and peripheral arterioles within the medullary canal. The descending artery also branches into central and peripheral arterioles, each giving rise to approximately four or five smaller arteries as they approach the distal tibia (Figure 1A). Along their course in the shaft the smaller arteries give off winding, thin branches at intervals passing to cortical bone through horizontal canals known as Volkmann's canals (Figure 1B). The vessels gradually divide into capillaries and anastomose with sinusoids. The great majority of sinusoids are located along the medullary rim and converge horizontally to form collecting sinusoids, which empty into the central vein (Figure 1C). The central vein accompanies the nutrient artery out of the nutrient foramen (Figure 1A). Three types of sinusoids were identified: a granular type, a short tubular type, and a grapeform type (Figure 1D–E). The epiphyses are richly vascularized with abundant capillaries, but only with a few sinusoids (Figure 1F). Circular impressions of sphincters in the surface of capillaries (Figure 1D) and endotheliocyte indentations in the surface of casts from sinusoids and arterioles were clearly displayed (Figure 2). In only 1 of 9 normal limbs, a shunting capillary was found. It emptied directly from an arteriole into a collecting sinusoid without passing the blood through sinusoids.

Figure 1. Scanning electron microscopy of microvascular corrosion casts of rabbit tibiae. Normal bone.

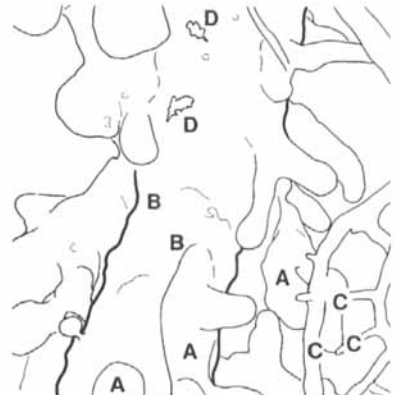
A. Intramedullary microvascular system with major branch from the nutrient artery (A), smaller arterial branch (B), central vein (C), and capillary branches (D), x50.



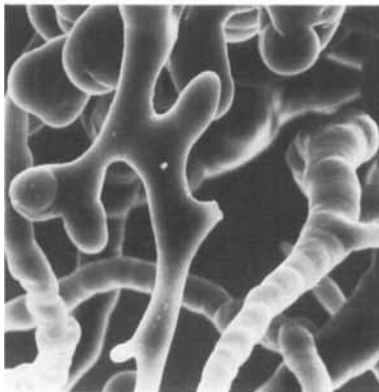
B. Profile of meshed microvascular cast from endosteal surface of cortical bone with sinusoid (A), Volkmann's canals (B), and artery with circular impressions (C), x200.

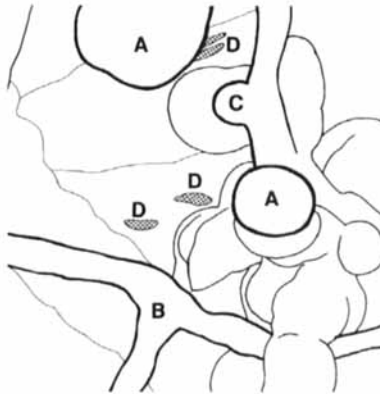
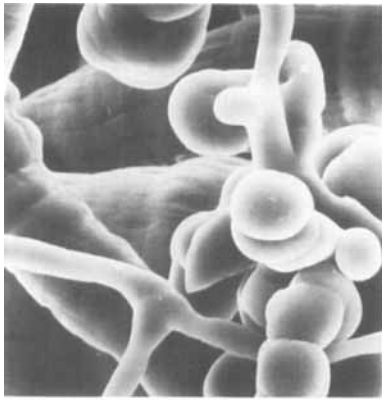


C. Collecting sinusoids (A) emptying into a central medullary vein (B) lined by capillaries (C). Small irregularities (D) on the surface of the central vein are artifacts, x300.

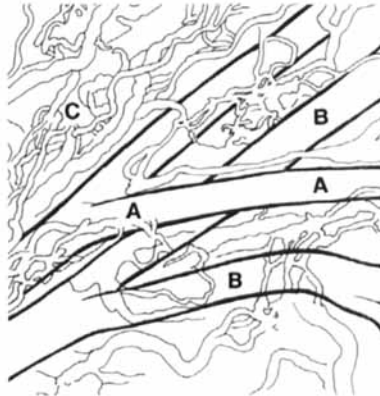
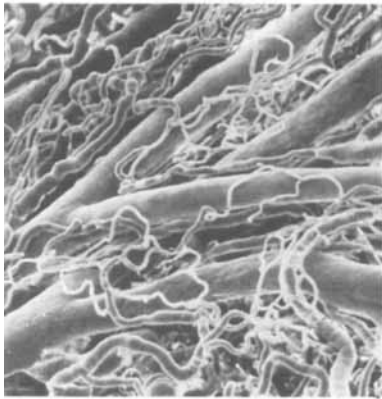


D. Granular and short tubular types of sinusoids (A). Arteriolar branches with circular sphincter-like impressions (B). Presumably incomplete filling of small sinusoid branch (C), x600.





E. Grapeform sinusoids (A) and a branching capillary (B). Presumably incomplete sinusoid filling (C). Impressions of endothelial cells into wall of artery (D), x600.



F. Cast from the richly vascularized tibial epiphysis with arterioles (A), venoles (B), and abundant capillaries (C). Note the absence of sinusoids, x150.

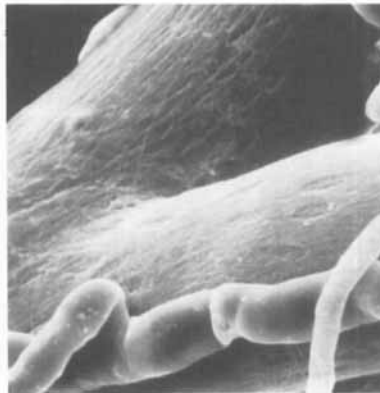


Figure 2. Endotheliocyte impressions in the surface of (left) a sinusoid cast (x2000) and (right) an arteriole (x700).

Arthrosis (Figure 3). In the immobilized extremity the normal sinusoid shape disappeared. Significant changes appeared in all immobilized tibiae. The main features were leakage of casting material from medullary rim sinusoids (Figure 3A), disappearance of the smooth surface of sinusoids and appearance of rough-surfaced sinusoids (Figures 3B, C). Shunting capillaries with a diameter of about 10–15 microns were found in eight of nine immobilized legs (Figures 3C, D).

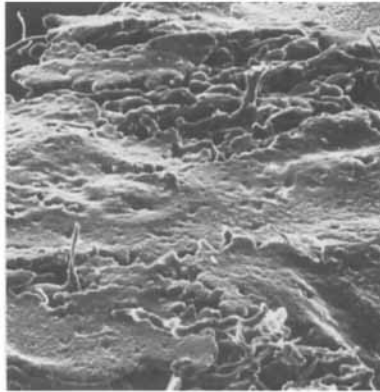
Discussion

Corrosion casting is a well-established method for studies of the anatomy of vessels and anatomic cavities. Murakami (1971) was the first to use scanning electron microscopy to analyze microvascular corrosion casts. This technique is capable of producing very detailed three-dimensional images of the intact microvasculature. Technical aspects of the method and the international literature on its use in normal and pathologic states in various tissues have recently

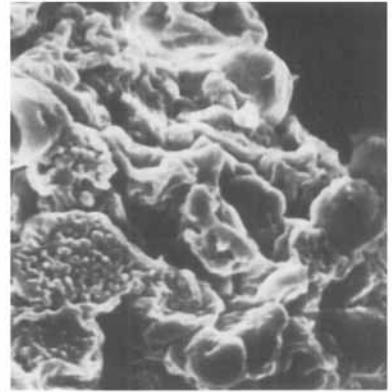
Figure 3. Scanning electron microscopy of intraosseous microvascular corrosion casts from immobilized rabbit tibiae.

A. Leakage of vascular cast material from sinusoids near the metaphyseal bone surface, $\times 30$.

B. Leakage of cast material and appearance of rough-surfaced sinusoids, $\times 500$.



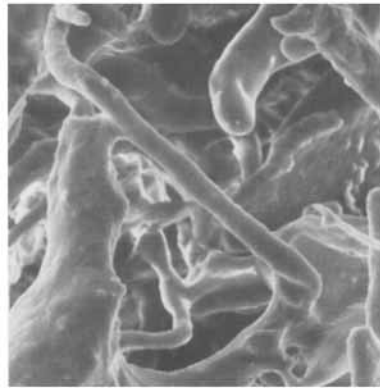
A



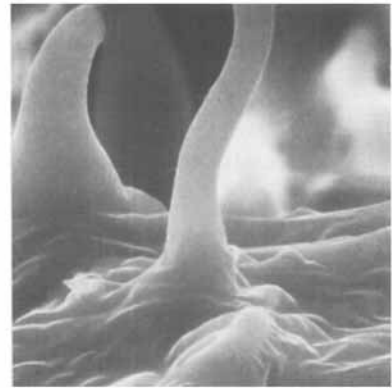
B

C. Dilated rough sinusoids with shunting capillary connecting collecting sinusoids, $\times 200$.

D. Sinusoids and shunting capillary on the central vein, $\times 1500$.



C



D

been reviewed exhaustively (Lametschwandner et al. 1984). The method has previously been employed for studies on the microvascular anatomy of normal bone and especially bone marrow (Irina et al. 1975, Draenert and Draenert 1980a, b, Jakob et al. 1980, Ohtani 1982). The present study appears to be the first to employ the method in pathologic bone.

We used the experimental model of arthrosis according to Videmann's (1982) method and achieved moderate arthrotic changes similar to those previously reported. A variety of factors may be responsible for the bone changes in this model. Osteophyte formation might reflect a chronic change in the hemodynamics of the arthrotic epiphysis, where venous engorgement results in intermittent ischemia with increased $p\text{CO}_2$, and decreased $p\text{O}_2$ and pH (Pedersen et al. 1988). Immobilization of the joint in extension causes stretching of the posterior capsule, which impairs the blood circulation, particularly in the proximal tibia. In addition, synovial inflamma-

tion and effusion may cause intramedullary venous stasis and intraosseous hypertension (Bünger et al. 1982). Another mechanism of arthrosis might be that capsular thickening and shortening, as well as muscle contraction, increase the compression on articular cartilage causing primary cartilage damage (Videmann 1982).

Whether the microvascular changes initiate the degenerative joint disease is still an open question. Because bone is a relatively incompressible structure, changes in venous-outlet resistance must cause intraosseous hypertension. Persistent intraosseous venous stasis may lead to intramedullary microcirculatory failure and subsequently metabolic changes characterized by lactic acid accumulation, hypoxia and hypercapnia (Holm et al. 1990).

The present morphologic study demonstrated outstanding differences between immobilized bone and control bone. The microvascular casts from arthrotic bone were characterized by rupture of sinusoids, collecting sinusoid leakage, and destruction of the

normal sinusoid surface. Shunting capillaries from arterioles to collecting sinusoids or the central vein were found in 8 rabbits. Thus, long-term intramedullary venous stasis may lead to arteriovenous shunting and cause a redistribution of normal blood flow which could leave the arthrotic bone without sufficient nutrient blood supply. The clinical demonstration of venous engorgement in arthrotic bone (Brookes 1968) and in other experimental investigations of arthrosis (Termansen et al. 1981, Hungerford 1981, Christensen 1985), together with the present findings, strongly suggest that arthrosis can be promoted by venous congestion resulting in impeded microcirculation. The endotheliocyte of the sinusoids may subsequently degenerate causing sinusoid leakage and destruction. Secondly, the bone metabolism will be impaired, and focal bone necrosis may occur.

This paper has provided evidence for major changes in bone sinusoid structure in arthrosis, which may explain the development of some of the bone lesions seen in arthrosis.

Acknowledgements

This study was supported by the Science Foundation from Henan Medical University. The expert technical assistance provided by Liu Bao-min is gratefully acknowledged.

References

- Arnoldi C C, Linderholm H, Muussbichler H. Venous engorgement and intraosseous hypertension in osteoarthritis of the hip. *J Bone Joint Surg (Br)* 1972; 54: 409-21.
- Arnoldi C C, Reimann I. The pathomechanism of human coxarthrosis. *Acta Orthop Scand* 1979; 50(Suppl 181): 1-47.
- Brookes M, Helal B. Primary osteoarthritis, venous engorgement and osteogenesis. *J Bone Joint Surg (Br)* 1968; 50(3): 493-504.
- Bünger C, Harving S, Bünger E H. Intraosseous pressure in the patella in relation to simulated joint effusion and knee position: an experimental study in puppies. *Acta Orthop Scand* 1982; 53(5): 745-51.
- Christensen S B. Osteoarthrosis. Changes of bone, cartilage and synovial membrane in relation to bone scintigraphy. *Acta Orthop Scand* 1985; 56 (Suppl 214) : 1-43.
- Draenert K, Draenert Y. The vascular system of bone marrow. *Scan Electron Microsc* 1980(4): 113-22.
- Draenert K, Draenert Y. Die Gefäßversorgung langer Röhrenknochen. Ihre Architektur in Beziehung zu den Knochenbälchen und Kanälen. *Beitr Elektronmikroskop Direktabbildn Oberfl* 1980; 13: 317-24.
- Finsterbush A, Friedman B. Reversibility of joint changes produced by immobilization in rabbits. *Clin Orthop* 1975; 111: 290-8.
- Harrison M H M, Schajowicz F, Trueta J. Osteoarthritis of the hip: A study of the nature and evolution of the disease. *J Bone Joint Surg (Br)* 1953; 35: 598-626.
- Holm I E, Ewald H, Bülow J, Bünger C. Vasoactive substances in subchondral bone of the dog knee. *J Orthop Res* 1990; 8(2): 205-12.
- Hungerford D S. Pathogenetic considerations in ischemic necrosis of bone. *Can J Surg* 1981; 24(6): 583-90.
- Irino S, Ono T, Watanabe K, Toyota K, Uno J, Takasugi N, Murakami T. SEM Studies of microvascular architecture, sinus wall, and transmural passage of blood cells in the bone marrow by a new method of injection replica and non-coated specimens. *Scan Electron Microsc* 1975(1): 267-74.
- Jakob H, Tosch U, Draenert K. Untersuchungen zur Gefäßversorgung der Wachstumsfuge. Teil I. *Beitr Elektronmikroskop Direktabbildn Oberfl* 1980; 13: 325-30.
- Lametschwandtner A, Lametschwandtner U, Weiger T. Scanning electron microscopy of vascular corrosion casts technique and applications. *Scan Electron Microsc* 1984; (Pt 2): 663-95.
- Langenskiöld A, Michelsson J E, Videman T. Osteoarthritis of the knee in the rabbit produced by immobilization. Attempts to achieve a reproducible model for studies on pathogenesis and therapy. *Acta Orthop Scand* 1979; 50(1): 1-14.
- Murakami T. Application of the scanning electron microscope to the study of the fine distribution of the blood vessels. *Arch Histol Jpn* 1971; 32(5): 445-54.
- Murakami T. Methyl methacrylate injection replica method. In: *Principles and Techniques of Scanning Electron Microscopy* (Ed. Hayat M. A). Van Nostrand, New York 1978; 6: 159-69.
- Ohtani O, Gannon B, Ohtsuka A, Murakami T. The microvasculature of bone and especially of bone marrow as studied by scanning electron microscopy of vascular casts. A review. *Scan Electron Microsc* 1982; (Pt 1): 427-34.
- Pedersen N W, Kiaer T, Kristensen K D, Starklint H. Intraosseous hydrostatic pressure and pO₂ in early nontraumatic necrosis of the femoral head. *Acta Orthop Scand* 1988; 59(Suppl 227): 12.
- Telhag H, Lindberg L. A method for inducing osteoarthritic changes in rabbits' knees. *Clin Orthop* 1972; 86: 214-23.
- Termansen N B, Teglbjaerg P S, Sørensen K H. Primary osteoarthritis of the hip. Interrelationship between intraosseous pressure, X-ray changes, clinical severity and bone density. *Acta Orthop Scand* 1981; 52(2): 215-22.
- Videman T. Experimental osteoarthritis in the rabbit: comparison of different periods of repeated immobilization. *Acta Orthop Scand* 1982; 53(3): 339-47.